

PUBLISHED VERSION

Bowman, Patrick Oswald; Heller, Urs M.; Leinweber, Derek Bruce; Parappilly, Maria Betsy; Williams, Anthony Gordon

[Unquenched gluon propagator in Landau gauge](#) Physical Review D, 2004; 70(3):034509

© 2004 American Physical Society

<http://link.aps.org/doi/10.1103/PhysRevD.70.034509>

PERMISSIONS

<http://publish.aps.org/authors/transfer-of-copyright-agreement>

“The author(s), and in the case of a Work Made For Hire, as defined in the U.S. Copyright Act, 17 U.S.C.

§101, the employer named [below], shall have the following rights (the “Author Rights”):

[...]

3. The right to use all or part of the Article, including the APS-prepared version without revision or modification, on the author(s)' web home page or employer's website and to make copies of all or part of the Article, including the APS-prepared version without revision or modification, for the author(s)' and/or the employer's use for educational or research purposes.”

11th April 2013

<http://hdl.handle.net/2440/18064>

Unquenched gluon propagator in Landau gauge

Patrick O. Bowman,^{1,2} Urs M. Heller,³ Derek B. Leinweber,¹ Maria B. Parappilly,¹ and Anthony G. Williams¹
¹*Special Research Centre for the Subatomic Structure of Matter and The Department of Physics, University of Adelaide,
 SA 5005, Australia*

²*Nuclear Theory Center, Indiana University, Bloomington, Indiana 47405, USA*

³*American Physical Society, One Research Road, Box 9000, Ridge, New York 11961-9000, USA*

(Received 12 March 2004; published 19 August 2004)

Using lattice quantum chromodynamics (QCD) we perform an unquenched calculation of the gluon propagator in Landau gauge. We use configurations generated with the AsqTad quark action by the MILC collaboration for the dynamical quarks and compare the gluon propagator of quenched QCD (i.e., the pure Yang-Mills gluon propagator) with that of 2+1 flavor QCD. The effects of the dynamical quarks are clearly visible and lead to a significant reduction of the nonperturbative infrared enhancement relative to the quenched case.

DOI: 10.1103/PhysRevD.70.034509

PACS number(s): 12.38.Gc, 11.15.Ha, 12.38.Aw, 14.70.Dj

I. INTRODUCTION

The gluon propagator, the most basic quantity of QCD, has been the subject of much calculation and speculation since the origin of the theory. In particular there has long been interest in the infrared behavior of the Landau gauge gluon propagator as a probe into the mechanism of confinement [1]. Some authors have argued it to be infrared finite [2–4] while others favored it as infrared singular [5,6]. There is a long history of its study on the lattice, in quenched QCD [7–19] and in quenched SU(2) [20,21]. The restriction to quenched lattice gauge theory calculations has been due to the lack of sufficient computational resources. The quenched theory differs from full QCD only in the relative weighting of the background gauge configurations (due to the fermion determinant), but the evaluation of the Green's functions is otherwise the same. In the quenched approximation the fermion determinant is replaced by unity and this corresponds to the complete suppression of all quark loops. The removal of quark loops is equivalent to the limit where all sea-quark masses are taken to infinity. In this paper, we report the first results for the gluon propagator from an unquenched lattice computation.

We study the gluon propagator in Landau gauge using configurations generated by the MILC collaboration [22] available from the Gauge Connection [28]. These use “AsqTad” improved staggered quarks, giving us access to relatively light sea quarks. We find that the addition of dynamical quarks preserves the qualitative features of the gluon dressing function $q^2 D(q^2)$ in the quenched case—enhancement for intermediate infrared momenta followed by suppression in the deep infrared—but produces a clearly visible effect. A significant suppression of the infrared enhancement with respect to the quenched case is observed. It is interesting to compare these results to those of a recent Dyson-Schwinger equation study [23].

II. DETAILS OF THE CALCULATION

The gluon propagator is gauge dependent and we work in the Landau gauge for ease of comparison with other studies. It is also the simplest covariant gauge to implement on the

lattice. Landau gauge is a smooth gauge that preserves the Lorentz invariance of the theory, so it is a popular choice. It will be interesting to repeat this calculation for the Gribov-copy free Laplacian gauge, but that will be left for a future study.

The MILC configurations were generated with the $\mathcal{O}(a^2)$ one-loop Symanzik improved [24] Lüscher-Weisz gauge action [25]. The dynamical configurations use the “AsqTad” quark action, an $\mathcal{O}(a^2)$ Symanzik improved staggered fermion action. β and the bare sea-quark masses are matched such that the lattice spacing is held constant. The lattices we consider all have the same dimensions. This means that all systematics are fixed; the only variable is the addition of quark loops. The parameters are summarized in Table I. The lattice spacing is approximately 0.125 fm [26].

In Landau gauge the gluon propagator is entirely transverse. In Euclidean space, in the continuum, the gluon propagator has the tensor structure

$$D_{\mu\nu}(q) = \left(\delta_{\mu\nu} - \frac{q_\mu q_\nu}{q^2} \right) D(q^2), \quad (1)$$

and at tree level

$$D(q^2) = \frac{1}{q^2}. \quad (2)$$

TABLE I. Lattice parameters used in this study. The dynamical configurations each have two degenerate light quarks (up/down) and a heavier quark (strange). In physical units the bare masses range from ~ 16 to ~ 79 MeV. The lattice spacing is $a \approx 0.125$ fm.

	Dimensions	β	Bare quark mass	Number of configurations
1	$20^3 \times 64$	8.00	quenched	192
2	$20^3 \times 64$	6.76	0.01, 0.05	193
3	$20^3 \times 64$	6.79	0.02, 0.05	249
4	$20^3 \times 64$	6.81	0.03, 0.05	212
5	$20^3 \times 64$	6.83	0.04, 0.05	337

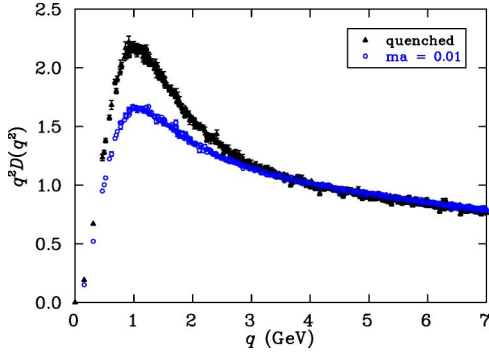


FIG. 1. Gluon dressing function in Landau gauge. Full triangles correspond to the quenched calculation, while open circles correspond to 2+1 flavor QCD. As the lattice spacing and volume are the same, the difference between the two results is entirely due to the presence of quark loops. The renormalization point is at $\mu = 4$ GeV. Data have been cylinder cut [16].

With this lattice gauge action the propagator at tree level is

$$D^{-1}(p_\mu) = \frac{4}{a^2} \sum_\mu \left\{ \sin^2\left(\frac{p_\mu a}{2}\right) + \frac{1}{3} \sin^4\left(\frac{p_\mu a}{2}\right) \right\}, \quad (3)$$

where

$$p_\mu = \frac{2\pi n_\mu}{aL_\mu}, \quad n_\mu \in \left(-\frac{L_\mu}{2}, \frac{L_\mu}{2} \right], \quad (4)$$

a is the lattice spacing and L_μ is the length of the lattice in the μ direction. As explained in Ref. [14], this suggests a “kinematic” choice of momentum,

$$q_\mu(p_\mu) \equiv \frac{2}{a} \sqrt{\sin^2\left(\frac{p_\mu a}{2}\right) + \frac{1}{3} \sin^4\left(\frac{p_\mu a}{2}\right)}, \quad (5)$$

ensuring that the lattice gluon propagator has the correct tree-level behavior.

The bare gluon propagator $D(q)$ is related to the renormalized propagator $D_R(q; \mu)$ through

$$D(q) = Z_3(\mu, a) D_R(q; \mu), \quad (6)$$

where μ is the renormalization point. In a renormalizable theory such as QCD, renormalized quantities become independent of the regularization parameter in the limit where it is removed. Z_3 is then defined by some renormalization prescription. We choose the momentum space subtraction (MOM) scheme where $Z_3(\mu, a)$ is determined by imposing the renormalization condition

$$D_R(q)|_{q^2=\mu^2} = \frac{1}{\mu^2}, \quad (7)$$

i.e., it takes the tree-level value at the renormalization point. In the following figures we have chosen $\mu = 4$ GeV.

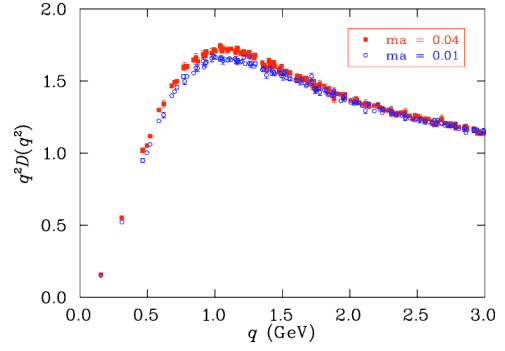


FIG. 2. The sea-quark mass dependence of the Landau gauge gluon propagator dressing function renormalized at $\mu = 4$ GeV. Filled squares correspond to u and d bare masses ≈ 63 MeV and bare s -quark mass ≈ 79 MeV. Open circles correspond to the same strange-quark mass, but with bare u and d masses ≈ 16 MeV. Data have been cylinder cut [16]. Increasing the sea-quark masses alters the results in the expected way, i.e., towards the quenched data.

III. SIMULATIONS RESULTS

Lattice studies strongly suggest that the quenched gluon propagator is infrared finite [14]. As is customary, we will begin by considering the (necessarily finite) gluon dressing function, $q^2 D(q^2)$. In Fig. 1 we compare the well-known quenched dressing function with that for 2+1 flavor QCD. For the moment we only consider the lightest of our dynamical quarks as we expect that they will show the greatest difference from the quenched case.

Indeed there is a clear difference between quenched and dynamical quark behavior in the infrared region. The addition of quark loops to the gluon propagator softens the infrared enhancement without altering its basic features. The screening of dynamical sea quarks brings the 2+1 flavor results significantly closer to the tree-level form, $q^2 D(q^2) = 1$.

In Fig. 2 we show the gluon dressing function for the lightest and for the heaviest u and d quark masses in our set. These correspond to bare light-quark masses of ≈ 16 MeV and ≈ 63 MeV, respectively; a factor of four difference. The bare strange-quark mass is the same in both cases (≈ 79 MeV). The mass dependence of the gluon dressing function is only just detectable. We expect that increasing the

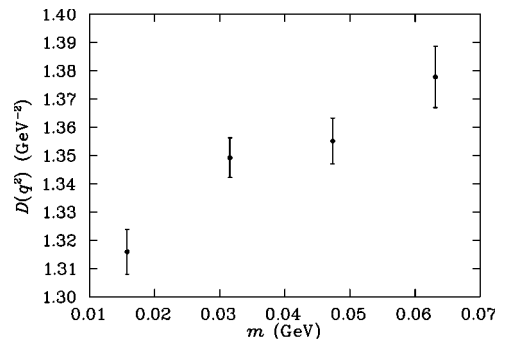


FIG. 3. The renormalized propagator at one momentum point in the infrared hump of the gluon dressing function ($q \approx 1.12$ GeV) is shown here as a function of the bare light-quark mass.

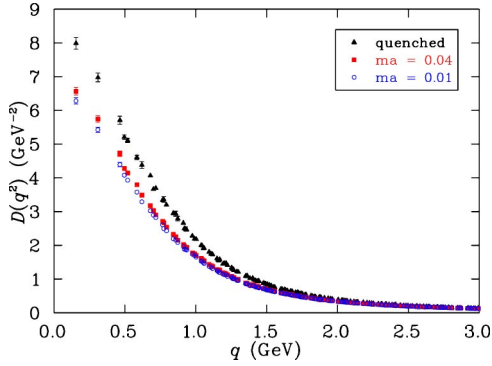


FIG. 4. The sea-quark mass dependence of the Landau gauge gluon propagator renormalized at $\mu=4$ GeV. Filled triangles illustrate the quenched propagator while filled squares correspond to bare up/down masses ≈ 63 and bare strange-quark mass ≈ 79 MeV. Open circles correspond to lighter bare up/down masses ≈ 16 MeV but with the same strange quark mass. Data have been cylinder cut [16].

sea-quark masses further will interpolate between the curves in Fig. 1. We see that the gluon propagator changes in the expected way. As the sea-quark mass increases, the curve moves toward the quenched result. However, for the range of bare quark masses studied here the change is relatively small. This transition would be better studied with heavier sea quarks.

Another view of the mass dependence of the gluon propagator is provided in Fig. 3. We choose one data point from the infrared hump ($q \approx 1.12$ GeV) and plot it for each choice of bare light-quark mass. Although the variation in the propagator at this momentum is only 4.5% over the range of quark masses investigated here, the light sea-quark mass dependence is clearly resolved.

In Fig. 4 we present results for the gluon propagator, $D(q^2)$. The largest effects of unquenching are observed in the deep infrared. The shape of the curves suggest that previous results indicating the infrared-finite nature of the quenched gluon propagator [14] are unchanged upon unquenching. The results suggest that the gluon propagator of QCD is infrared finite. It will be interesting to examine the behavior of $D(0)$ as a function of volume to elucidate this aspect of the gluon propagator further.

Finally, in Fig. 5 the light sea-quark mass dependence of the renormalized gluon propagator is illustrated for a momentum point in the infrared region. To avoid finite volume artifacts, the second smallest nontrivial momentum is considered. Whereas the mass dependence of the propagator for the masses studied here is at the 4.5% level for $q \approx 1.12$ GeV, the variance is larger in the infrared region at 6% for $q \approx 0.31$ GeV.

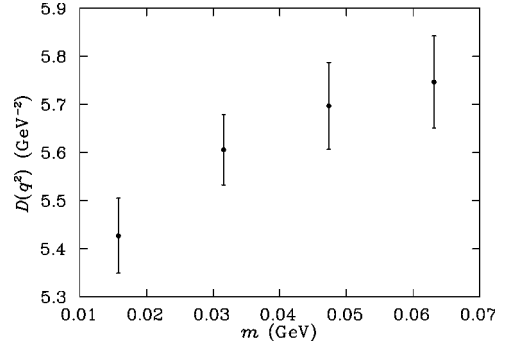


FIG. 5. The light sea-quark mass dependence of the renormalized gluon propagator at a momentum point in the infrared region ($q \approx 0.31$ GeV).

In a recent Dyson-Schwinger equation (DSE) study [23,27] the inclusion of the quark DSE in the gluon DSE was found to slightly diminish its infrared enhancement. Osterwalder-Schrader positivity is still violated. Our results are consistent with the qualitative features of that prediction.

IV. CONCLUSIONS

The addition of quark loops has a clear, quantitative effect on the gluon propagator. While its basic structure is qualitatively similar there is significant screening of the propagator in the infrared. As anticipated, the effect is to suppress the non-Abelian enhancement of the gluon propagator in the nonperturbative infrared-momentum region. This is relevant to analytic studies of the gluon propagator and confinement [23]. Despite the clear difference between the quenched and dynamical results, we see little dependence on the dynamical quark mass for the range of available light sea-quark masses. The dependence that is observed is consistent with expectations.

Calculations on finer lattices are currently being made, which will provide more information on the ultraviolet nature of the propagator and provide a test for finite lattice spacing artifacts. We would like to extend the study to a wider range of dynamical masses to study both the chiral limit and the transition to the quenched limit. Finally, a study of the volume dependence of the propagator will provide valuable insights into the nature of the propagator at $q^2=0$.

ACKNOWLEDGMENT

This research was supported by the Australian Research Council and by grants of time on the Hydra Supercomputer, supported by the South Australian Partnership for Advanced Computing.

[1] J.E. Mandula, hep-lat/9907020 (1998).

[2] V.N. Gribov, Nucl. Phys. **B139**, 1 (1978).

[3] M. Stingl, Phys. Rev. D **34**, 3863 (1986).

[4] D. Zwanziger, Nucl. Phys. **B364**, 127 (1991).

[5] S. Mandelstam, Phys. Rev. D **20**, 3223 (1979).

[6] K. Buttner and M.R. Pennington, Phys. Rev. D **52**, 5220 (1995).

[7] J.E. Mandula and M. Ogilvie, Phys. Lett. B **185**, 127 (1987).

- [8] C.W. Bernard, C. Parrinello, and A. Soni, *Phys. Rev. D* **49**, 1585 (1994).
- [9] P. Marenzoni, G. Martinelli, and N. Stella, *Nucl. Phys.* **B455**, 339 (1995).
- [10] J.P. Ma, *Mod. Phys. Lett. A* **15**, 229 (2000).
- [11] D. Becirevic *et al.*, *Phys. Rev. D* **60**, 094509 (1999).
- [12] D. Becirevic *et al.*, *Phys. Rev. D* **61**, 114508 (2000).
- [13] H. Nakajima and S. Furui, *Nucl. Phys.* **A680**, 151 (2000).
- [14] F.D.R. Bonnet, P.O. Bowman, D.B. Leinweber, A.G. Williams, and J.M. Zanotti, *Phys. Rev. D* **64**, 034501 (2001).
- [15] K. Langfeld, H. Reinhardt, and J. Gattnar, *Nucl. Phys.* **B621**, 131 (2002).
- [16] D.B. Leinweber, J.I. Skullerud, A.G. Williams, and C. Parrinello, *Phys. Rev. D* **60**, 094507 (1999).
- [17] D.B. Leinweber, J.I. Skullerud, A.G. Williams, and C. Parrinello, *Phys. Rev. D* **58**, 031501 (1998).
- [18] P.O. Bowman, U.M. Heller, D.B. Leinweber, and A.G. Williams, *Phys. Rev. D* **66**, 074505 (2002).
- [19] F.D.R. Bonnet, P.O. Bowman, D.B. Leinweber, and A.G. Williams, *Phys. Rev. D* **62**, 051501(R) (2000).
- [20] A. Cucchieri, *Phys. Lett. B* **422**, 233 (1998).
- [21] A. Cucchieri, T. Mendes, and A.R. Taurines, *Phys. Rev. D* **67**, 091502(R) (2003).
- [22] C.W. Bernard *et al.*, *Phys. Rev. D* **64**, 054506 (2001).
- [23] R. Alkofer, W. Detmold, C.S. Fischer, and P. Maris, *Phys. Rev. D* **70**, 014014 (2004).
- [24] K. Symanzik, *Nucl. Phys.* **B226**, 187 (1983).
- [25] M. Luscher and P. Weisz, *Chem. Phys.* **97**, 59 (1985); **98**, 433(E) (1985).
- [26] HPQCD, C.T.H. Davies *et al.*, *Phys. Rev. Lett.* **92**, 022001 (2004).
- [27] C. Fischer and R. Alkofer, *Phys. Rev. D* **67**, 094020 (2003).
- [28] <http://www.qcd-dmz.nersc.gov>